A Multiphase Strategy for Realizing Green Cathodoluminescence in 12CaO·7Al2O3−CaCeAl3O7:Ce3+,Tb3+ Conductive Phosphor

Xiuling Liu
Northeast Normal University

Yuxue Liu
Northeast Normal University

Duanting Yan
Northeast Normal University

Hancheng Zhu
Northeast Normal University

Chunguang Liu
Northeast Normal University

See next page for additional authors

Follow this and additional works at: https://digitalcommons.georgiasouthern.edu/physics-facpubs

Part of the Physics Commons

Authors

Xiuling Liu, Yuxue Liu, Duanting Yan, Hancheng Zhu, Chunguang Liu, Weizhen Liu, Changshan Xu, Yichun Liu, Hong Zhang, and Xiao-Jun Wang

PAPER

A multiphase strategy for realizing green cathodoluminescence in $12CaO \cdot 7Al_2O_3$–$CaCeAl_3O_7$: Ce^{3+},Tb^{3+} conductive phosphor

Xiuling Liu,[a] Yuxue Liu,*[a] Duanting Yan,[a] Hancheng Zhu,[a] Chunguang Liu,[a] Weizhen Liu,[a] Changshan Xu,[a] Yichun Liu,[a] Hong Zhang*[b] and Xiaojun Wang*[c]

A multiphase strategy is proposed and successfully applied to make the insulating green phosphor $CaCeAl_3O_7:Tb^{3+}$ conductive in the form of $12CaO \cdot 7Al_2O_3$–$CaCeAl_3O_7:Ce^{3+},Tb^{3+}$. The phosphor shows bright green-light emission with a short lifetime (2.51 ms) under low-voltage electron beam excitation (3 kV). The green photo- and cathodoluminescence from $^5D_4$–^7F_J (J = 6, 5, 4, 3) transitions of Tb^{3+} are significantly enhanced in comparison with pure $C12A7:Tb^{3+}$. It was confirmed that this enhancement is the consequence of the joint effects of energy transfer from Ce^{3+} to Tb^{3+} and broadening of the absorption spectrum of Ce^{3+} due to the existence of multiple phases. In particular, under 800 V electron beam excitation, cathodoluminescence is improved by the modified electrical conductivity of the phosphor. When compared to the commercial $Zn_2SiO_4:Mn^{2+}$ with a long luminescence lifetime of 11.9 ms, this conductive green phosphor has greater advantage for fast displays.

1. Introduction

Field emission displays (FEDs) are widely regarded as one of the most promising technologies in flat panel displays, owing to their thin panels, self-emission, distortion-free image, wide viewing angle, low weight, quick response, and low power consumption.[1,2] FED technology requires that the phosphor be electrically conductive to avoid electron accumulation on the phosphor surface because of their lower electron accelerating voltage, typically 1–5 kV, than the phosphor used in a conventional cathode ray tube (CRT) screen. Although sulfide-based compounds have high efficiency and a suitable electrical conductivity, the volatility of sulfur has prohibited their application in FEDs.[3,4] Recently, increasing attention has been paid to new oxide-based phosphors because of their superior colour richness and good chemical and thermal stabilities compared to sulfides.[5–8] However, most oxide-based phosphors are wide band-gap insulators which have low electrical conductivity. To address this challenge, two general approaches have been

proposed. One is to choose appropriate band gap oxysalts, like germanates[9,10] which have reasonable conductivity. The main problem is their poor stability under low-voltage cathode-ray bombardment. The other approach is to coat or mix the insulating phosphors with a transparent and conductive oxide, such as SnO_2, In_2O_3, and ZnO.[11–13] The drawback of this approach is the high cost and complex preparation procedure. Furthermore, the conductive oxides have no contribution to luminescence. Therefore, there is a need to develop an economical approach for improving the conductivity of insulating oxide-based phosphors capable of adapting themselves to electron-beam bombardment.

Calcium aluminium oxide ($12CaO \cdot 7Al_2O_3$, abbreviated as $C12A7:O^{2-}$ or C12A7) is found to have unique physical and chemical properties based on its special crystal nanocage structure.[14–16] In this insulating compound, O^{2-} ions are caged species that compensate for the positive charge of the ~0.4 nm cage and the electrical conductivity can be improved simply by replacing these anions with electrons.[17,18] Electrons can be readily introduced into the cages by means of various chemical and physical processes. For example, Hosono *et al.* have converted C12A7 from an insulator into a semiconductor by doping with H^- ions followed by irradiation with ultraviolet (UV) light or an electron beam.[19,20] In addition, we have achieved bright green emission through efficient energy transfer in Ce^{3+}, Tb^{3+} co-doped $C12A7:O^{2-}$ phosphors with UV light excitation.[21] The main problem with these phosphors is their poor conductivity.

In this paper, we propose a new strategy for making insulating oxide phosphors conductive by introducing a conductive

[a]*Center for Advanced Optoelectronic Functional Materials Research & Key Laboratory for UV Light-Emitting Materials and Technology of the Ministry of Education, Northeast Normal University, 5268 Renmin Street, Changchun 130024, China. E-mail: yxliu@nenu.edu.cn*

[b]*Van't Hoff Institute for Molecular Sciences, University of Amsterdam, P.O. Box 94157, 1090 GD Amsterdam, The Netherlands. E-mail: H.Zhang@uva.nl*

[c]*Department of Physics, Georgia Southern University, Statesboro, GA 30460-8031, USA. E-mail: xwang@georgiasouthern.edu; Fax: +1-912-478-0471; Tel: +1-912-478-5503*

phase. Applying this so-called multiphase approach, we have successfully prepared conductive C12A7-CaCeAl$_3$O$_7$:Ce^{3+},Tb^{3+} as a candidate for green-light-emitting phosphors by solid-state reactions. It is found that phase-mixing can not only improve significantly the conductivity of the phosphor, but also enhance the cathodoluminescence (CL). The conductive phosphor can emit a reasonably strong green-light emission even when the voltage is lowered to 800 V. On top of that, the lifetime of the emission is short (2.51 ms), which makes this material attractive for application in FEDs. Relevant mechanisms are also explored in this work.

2.   Experimental

C12A7:Ce^{3+},Tb^{3+} and multiphased C12A7-CaCeAl$_3$O$_7$:Ce^{3+},Tb^{3+} powders were synthesized by solid-state reactions using CaCO$_3$ (99.99%), Al$_2$O$_3$ (99.99%), CeO$_2$ (99.99%), and Tb$_4$O$_7$ (99.99%) as the starting materials. The ingredients were quantitatively mixed, and then pre-fired at 850 °C in air for 2 hours. The pre-fired samples were thoroughly reground and subsequently calcined at 1350 °C in air for 8 hours. Then, the powders were annealed at 1300 °C under a reducing atmosphere of 20% H$_2$/80% N$_2$ for 6 hours (flow rate: 45 ml min^{-1}) to convert tetravalent terbium and cerium ions into the trivalent state and introduce the encaged H$^-$ ions (C12A7:H$^-$). The ratio of CaCeAl$_3$O$_7$ can be modified by varying the concentration of Ce^{3+}. To ensure that the multiphased samples are conductive, C12A7 is required to be the main phase, so that the nominal expression of samples is C12A7:x% Ce^{3+}, y% Tb^{3+}. For the purpose of simplicity, we still use the nominal expression C12A7:x% Ce^{3+}, y% Tb^{3+} to represent our multiphased samples in the following discussion.

X-ray diffraction (XRD) patterns were recorded using a Rigaku D/max-RA X-ray diffraction spectrometer with 2θ in the range of 10–80° using CuKα radiation (average line of 0.15418 nm). Crystal structure refinements were performed by the Rietveld method using the General Structure Analysis System (GSAS) software suite.[22] The morphology was characterized by scanning electronic microscopy (SEM, FEI, Quanta FEG 250). Diffuse reflectance spectra were recorded using a Lambda 900 UV/VIS/NIR spectrophotometer (Perkin Elmer, USA). The photoluminescence (PL) measurements were carried out using a Shimadzu RF-5301PC spectrofluorometer. The CL measurements were performed using a MonoCL4 system (Gatan UK) attached to an SEM, where the phosphors were excited by an electron beam. The luminescence decay curves were measured using an FLSP920 Edinburgh Fluorescence Spectrometer. All measurements were performed at room temperature.

3.   Results and discussion

Fig. 1 shows the XRD patterns of nominal C12A7:x% Ce^{3+}, y% Tb^{3+} (x = 0, 0.25, 0.5, 1.0, 3.0, 5.0 and y = 1.0). When x ≤ 0.5, all diffraction peaks are in good agreement with the standard
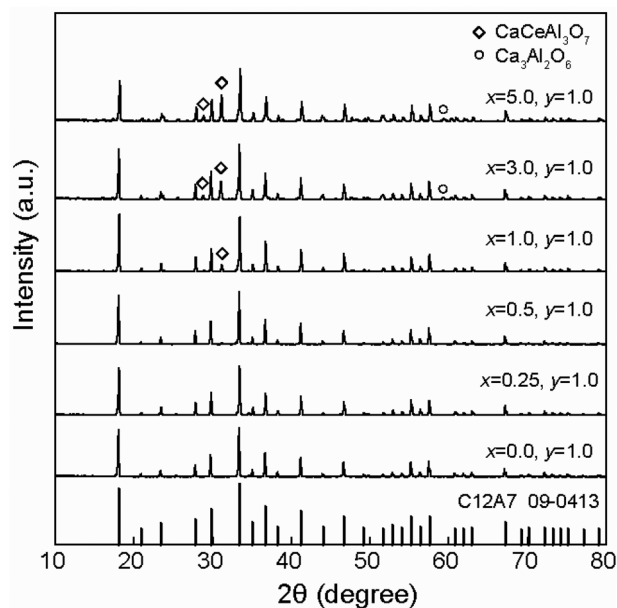

Fig. 1 XRD patterns of nominal C12A7:x% Ce^{3+}, 1.0% Tb^{3+} annealed at 1300 °C for 6 hours under a reducing atmosphere.

powder diffraction data (C12A7, JCPDS: 09-0413), indicating that cubic phase polycrystalline C12A7 powders are obtained. Ce^{3+} has an ionic radius of 1.03 Å and Tb^{3+} has 0.92 Å, both of which are much larger than that of Al^{3+} (0.39 Å, CN = 4). Therefore, it is reasonable to assume that Ce^{3+} and Tb^{3+} ions are preferentially substituted for Ca^{2+} ions with an equivalent radius (0.99 Å) in C12A7. When x > 0.5, except for all diffraction peaks of the standard powder diffraction data of C12A7, new peaks (such as 28.78° and 31.03°) appear in the samples, which are assigned to CaCeAl$_3$O$_7$ according to the Rietveld refinement as depicted in Fig. 2. It is found that the ratio of the CaCeAl$_3$O$_7$ phase gradually increases with increasing Ce^{3+} concentration, and multiphased samples with different phase ratios are obtained.

The black crosses and red lines in Fig. 2 represent the observed and calculated patterns, respectively, and the obtained goodness of fit parameter χ^2 = 5.94 and R_{wp} (13.07%) ensure the reliability of fitting. The sample contains C12A7, CaCeAl$_3$O$_7$ and Ca$_3$Al$_2$O$_6$, and their phase fractions are 74.2%, 17.7% and 8.1%, respectively. The phase fractions of CaCeAl$_3$O$_7$ are 4.3% and 17.8% for C12A7: 1.0% Ce^{3+}, 1.0% Tb^{3+} and C12A7: 5.0% Ce^{3+}, 1.0% Tb^{3+}, respectively. CaCeAl$_3$O$_7$ is one of the complex oxides in the rare earth calcium aluminate family with a general composition of ABC$_3$O$_7$, where A is an alkaline earth cation, B a yttrium, scandium or a trivalent rare earth element and C an aluminium, gallium or a transition metal ion. Rare earth ion doped ABC$_3$O$_7$ with excellent emissions have been studied widely, such as CaYAl$_3$O$_7$:Ce/Eu, CaGdAl$_3$O$_7$:Yb, and GdSrAl$_3$O$_7$:Yb,[23–25] which are insulating due to the wide band gap energy (~7 eV).[26] Thus, CaCeAl$_3$O$_7$:Tb^{3+} might exhibit strong green emission, in principle. Usually C12A7 might decompose into CaAl$_2$O$_4$ and Ca$_3$Al$_2$O$_6$
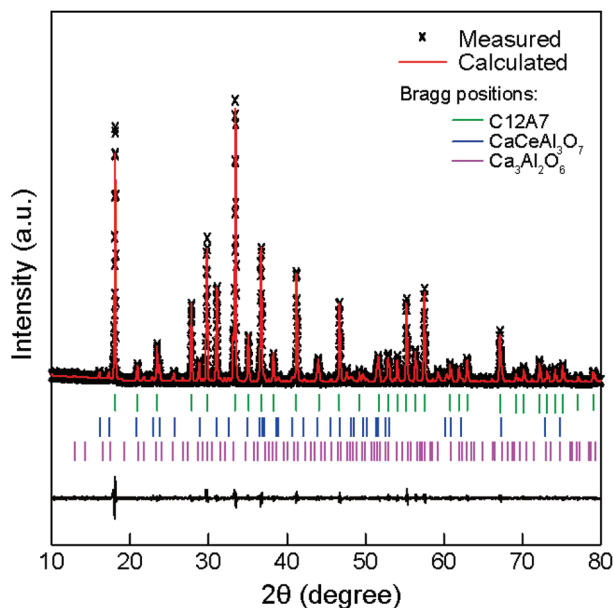
Fig. 2 Observed (crosses) and calculated (solid line) XRD patterns of the Rietveld refinement of C12A7:3.0% Ce^{3+}, 1.0% Tb^{3+} annealed at 1300 °C for 6 hours under a reducing atmosphere. Green, blue and purple vertical lines represent the positions of Bragg reflection of C12A7, $CaCeAl_3O_7$ and $Ca_3Al_2O_6$. The difference profile is plotted on the same scale in the bottom.

Fig. 3 Excitation (a, normalized) and emission spectra (b) of the C12A7:x% Ce^{3+}, 1.0% Tb^{3+} annealed at 1300 °C for 6 hours under a reducing atmosphere. The inset shows decay curves of Ce^{3+} under 355 nm excitation.

under a reducing atmosphere.[27] Herein, it is suggested that $CaCeAl_3O_7$ is generated by the following reaction:

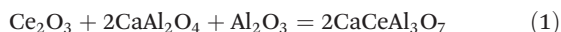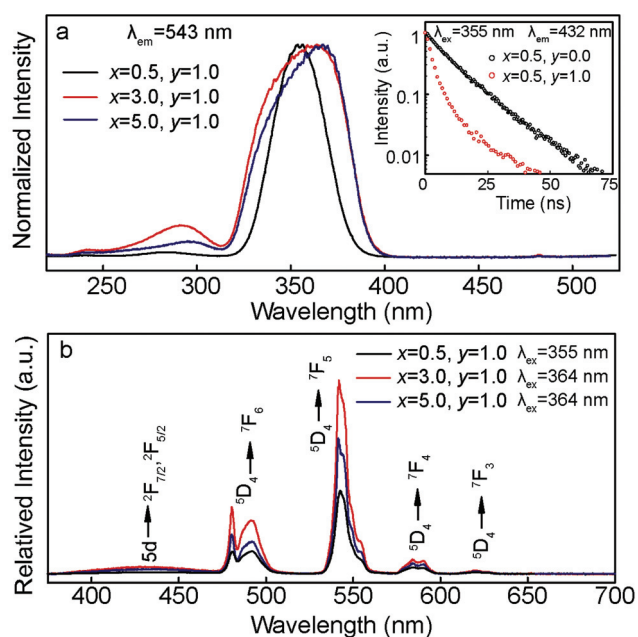$$Ce_2O_3 + 2CaAl_2O_4 + Al_2O_3 = 2CaCeAl_3O_7 \qquad (1)$$

Fig. 3 shows the emission and excitation spectra of C12A7:x% Ce^{3+}, y% Tb^{3+} annealed at 1300 °C for 6 hours under a reducing atmosphere of 20% H_2/80% N_2. When the emission of Tb^{3+} at 543 nm ($^5D_4 \rightarrow ^7F_5$) is monitored, broad absorption bands in the near UV region dominate the excitation spectra of all the codoped samples, attributed to the f–d transitions of Ce^{3+}.[28] The weak band centered at 240 nm could be due to the transitions from the ground state to the 5d energy levels of the Tb^{3+}. The dominating absorption band of Ce^{3+} in C12A7:3.0% Ce^{3+}, 1.0% Tb^{3+} (peaked at 364 nm) becomes broadened (FWHM changes from 33 to 53 nm), unsymmetrical, and redshifted compared to that of C12A7:0.5% Ce^{3+}, 1.0% Tb^{3+} (peaked at 355 nm) due to the increasing phase fraction of $CaCeAl_3O_7$. Chen et al. have reported that the excitation bands of $Ca_3Al_2O_6$:Ce^{3+} were located respectively at 330 and 339 nm.[29] Therefore, $CaCeAl_3O_7$ is believed to be responsible for the red shift and the broadening of the absorption band of Ce^{3+}.

In the efficient UV excitation region of Ce^{3+}, the phosphors emit bright green light that combines a weak broad band peaked at 432 nm, assigned to the 5d–4f transitions of Ce^{3+}, and several narrow bands centered at 492, 543, 584, and 620 nm, ascribed to the $^5D_4$–^7F_J (J = 6, 5, 4, 3) transitions of Tb^{3+}, respectively. The PL intensity of C12A7:3.0% Ce^{3+}, 1.0% Tb^{3+} is stronger than that of both C12A7:0.5% Ce^{3+}, 1.0% Tb^{3+} and C12A7:5.0% Ce^{3+}, 1.0% Tb^{3+} that has the broadest absorption band in all the prepared samples. To study the effect
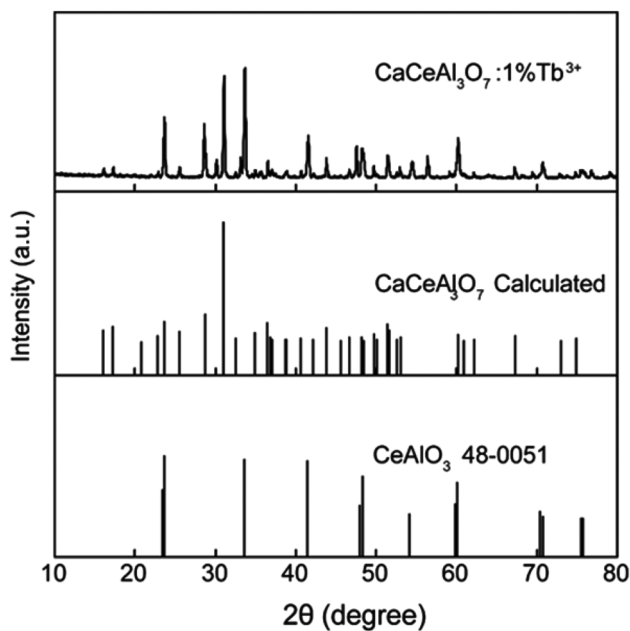
Fig. 4 XRD patterns of $CaCeAl_3O_7$:1% Tb^{3+} containing $CeAlO_3$ and the calculated $CaCeAl_3O_7$.

of $CaCeAl_3O_7$ on PL enhancement, we prepared a $CaCeAl_3O_7$:1.0% Tb^{3+} phosphor. The results show that the single phased $CaCeAl_3O_7$ is hard to be synthesized and the obtained sample has both $CaCeAl_3O_7$ and $CeAlO_3$ (Fig. 4), but $CeAlO_3$ has no contribution to PL because its energy band gap (3.26 eV) is smaller than the dominating excitation energy (3.54 eV).[30] The near UV absorption band of $CaCeAl_3O_7$:1.0%
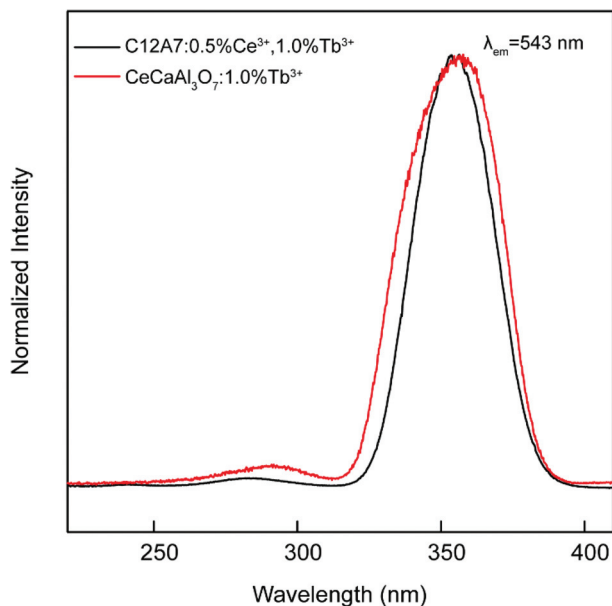
Fig. 5 Excitation spectra of CaCeAl$_3$O$_7$:1.0% Tb and C12A7:0.5% Ce^{3+}, 1.0% Tb^{3+} monitored at 543 nm.
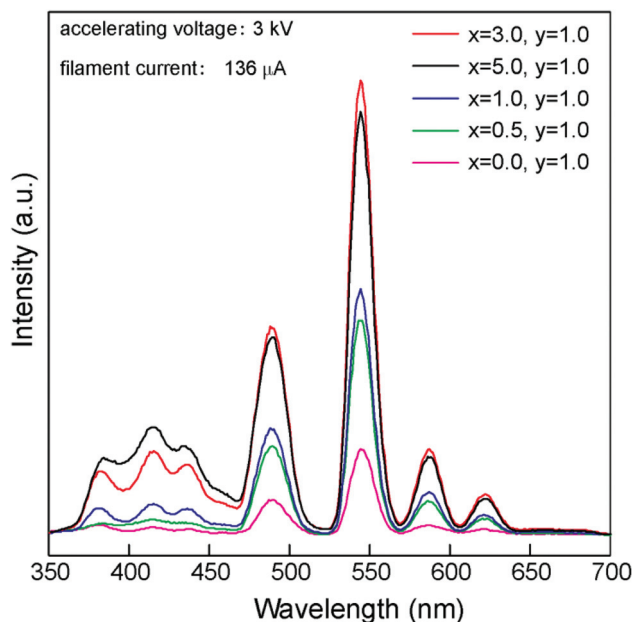
Fig. 6 CL spectra of C12A7:x% Ce^{3+}, 1.0% Tb^{3+} phosphors annealed at 1300 °C for 6 hours in a reducing atmosphere under low-voltage (3 kV) electron beam excitation.

Tb^{3+} is broader and red-shifted compared to pure C12A7:0.5% Ce^{3+}, 1.0% Tb^{3+} from the excitation spectra monitored at 543 nm (Fig. 5), which further proves that CaCeAl$_3$O$_7$ is responsible for the broadening of the absorption band of Ce^{3+} in the multiphased C12A7-CaCeAl$_3$O$_7$.

In our previous report, a significant spectral overlap has been observed between the emission band of C12A7:Ce^{3+} and the excitation band of C12A7:Tb^{3+}, making it possible to have an efficient energy transfer (ET) from Ce^{3+} to Tb^{3+}.[21] Here, the emission and excitation spectra demonstrate that the effective ET also occurs from Ce^{3+} to Tb^{3+} in the multiphased samples. As presented in Fig. 3, the emission of Tb^{3+} is observed upon excitation of Ce^{3+} and its intensity increases at higher concentrations of Ce^{3+}. To further prove the ET in C12A7, the luminescent decays of Ce^{3+} at room temperature in C12A7:0.5% Ce and C12A7:0.5% Ce, 1.0% Tb under 355 nm excitation have been measured, as shown in the inset of Fig. 3a. In singly Ce^{3+}-doped samples the decay shows a clear single-exponential pattern with a lifetime fitted to be 10.30 ns. In the C12A7:0.5% Ce, 1.0% Tb co-doped sample, the Ce^{3+} fluorescence decay becomes faster and demonstrates a bi-exponential, short component and a long component comparable with the singly doped Ce^{3+} sample, with lifetimes of 3.5 and 14.9 ns, respectively. This leads to the conclusion that some Ce^{3+} ions with Tb^{3+} in the close vicinity efficiently transfer the excitation Tb^{3+}, whereas others have no Tb^{3+} in the close neighborhood and thus the emission decay remains unchanged.

Fig. 6 shows the CL spectra of C12A7:x% Ce^{3+}, 1.0% Tb^{3+} phosphors annealed at 1300 °C for 6 hours under a reducing atmosphere of 20% H$_2$/80% N$_2$ under low-voltage (3 kV) electron beam excitation. The CL spectra are very similar to the PL emissions (Fig. 3b), except for three new narrow bands centred

at 380, 413, and 435 nm, which are ascribed to the $^5D_3$–^7F_J ($J =$ 6, 5, 4) transitions of Tb^{3+}, respectively. For PL, the UV excitation is efficient for Ce^{3+} and the transitions from $^5D_3$ of Tb^{3+} are very weak and submerged in the broad blue emission band of Ce^{3+}. For CL the primary fast and energetic electrons create many secondary electrons with a very broad excitation energy distribution, populating all the high-lying energy states, such as $^5D_3$, yielding the blue emissions. The CL of the multiphased samples is obviously stronger than that of the singly Tb^{3+} doped sample. The intensity increases visibly with the increase of the CaCeAl$_3$O$_7$ ratio and reaches the maximum at $x =$ 3.0, where the intensity is 5 times greater in comparison with C12A7:1.0% Tb^{3+}. The results indicate that effective ET from Ce^{3+} also enhances the Tb^{3+} emission under electron beam excitation. The strong CL enhancement partially results from the two phases mixing and the modified electrical conductivity of the samples.

Fig. 7 shows the CL spectra of C12A7:1.0% Tb^{3+}, CaCeAl$_3$O$_7$:1.0% Tb, and C12A7:3.0% Ce^{3+}, 1.0% Tb^{3+} phosphors annealed at 1300 °C for 6 hours under a reducing atmosphere under electron beam excitation (3 kV). CaCeAl$_3$O$_7$:1.0% Tb emits a broad band peaked at 400 nm assigned to the 5d–4f transitions of Ce^{3+} and several narrow bands centred at 492, 543, 584, and 620 nm, ascribed to the $^5D_4$–^7F_J transitions of Tb^{3+}. The CL intensity of C12A7:1.0% Tb^{3+} is weaker than that of CaCeAl$_3$O$_7$:1.0% Tb, indicating a higher luminescence efficiency of Tb^{3+} in CaCeAl$_3$O$_7$. Therefore, some Tb^{3+} ions enter the CaCeAl$_3$O$_7$ crystal lattice in the phase-mixed samples, and are responsible for the strong CL enhancement.

To study the relationship of the two factors, phase mixing and electrical conductivity, with CL enhancement, we changed
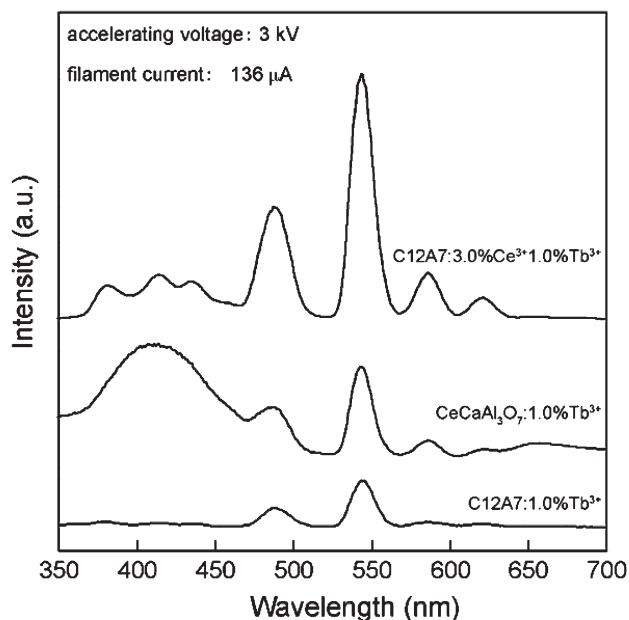
Fig. 7 The CL spectra of C12A7:1.0% Tb^{3+}, CaCeAl$_3$O$_7$:1% Tb^{3+}, and C12A7:3.0% Ce^{3+}, 1.0% Tb^{3+} phosphors annealed at 1300 °C for 6 hours under a reducing atmosphere under low-voltage (3 kV) electron beam excitation.
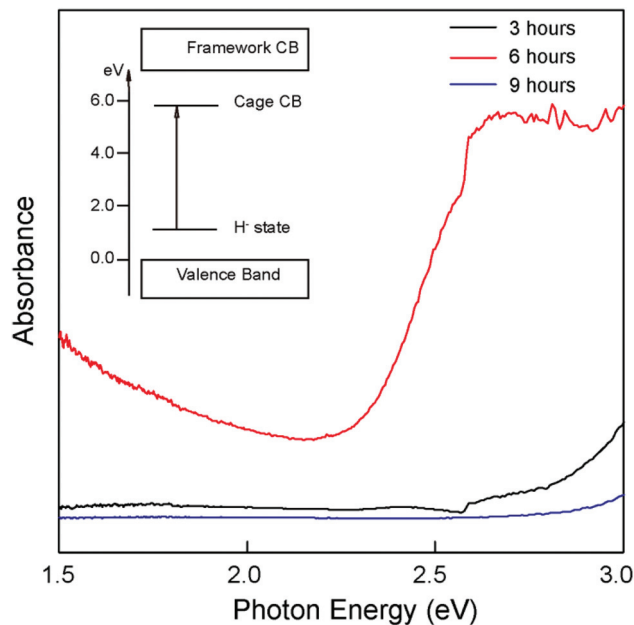

Fig. 8 The absorption spectra of C12A7:3.0% Ce^{3+}, 1.0% Tb^{3+} annealed at 1300 °C for different times (3, 6, and 9 hours).

the annealing time under a reducing atmosphere of C12A7:3.0% Ce^{3+}, 1.0% Tb^{3+} phosphors expecting to alter the electrical conductivity of the co-doped samples. Sushko *et al.* have considered that, for creating electrons, C12A7:H$^-$ is most sensitive to a wavelength around 300 nm (~4.1 eV), which corresponds to a charge-transfer transition from the encaged H$^-$ state to the cage conduction band (CCB) localized in the neighbouring cage,[31] as shown in the inset of Fig. 8. Hayashi *et al.* have further demonstrated that electron-beam irradiation also imparts an electrical conductivity to insulating H$^-$-doped C12A7.[19] Herein, C12A7:3.0% Ce^{3+}, 1.0% Tb^{3+} annealed for 6 hours under a H$_2$ atmosphere turns green and the optical absorption band centred at 2.75 eV appears after UV light irradiation (Fig. 8), indicating the conversion of the insulating C12A7 into an electronic conductor.[20] Our experimental results show that it is difficult to introduce H$^-$ into pure C12A7 by heat treatment under a H$_2$ atmosphere without rapidly cooling to room temperature.[32] However, the substitution of rare earth ions for divalent Ca^{2+} ions, due to their different valence and electronegativity values, may have affected the nanocage structure and induced more free O^{2-} ions, which are favourable for introducing H$^-$. For the sample annealed for 3 hours, there is only a small quantity of H$^-$ introduced into the cages, which is not enough to induce colour changes of the samples or to improve the electrical conductivity. For the sample annealed for 9 hours, almost all Ce^{3+} ions are separated out of C12A7 and turned into the phase of CaCeAl$_3$O$_7$, making H$^-$ entering C12A7 cages a difficult task. Consequently, C12A7:3.0% Ce^{3+}, 1.0% Tb^{3+} annealed for 6 hours under a H$_2$ atmosphere has an optimized electrical conductivity.

Fig. 9 shows the SEM image of C12A7:3.0% Ce^{3+}, 1.0% Tb^{3+} powders annealed for 6 hours under a reducing atmosphere without gold-plating. The clear image indicates that the sample has a good electrical conductivity without charge build-up. The slightly aggregated particles have a narrow size range of 2.8–4.3 μm, which is perfect to produce a compact phosphor screen and thus improve its CL property.

As shown in Fig. 10, the CL of C12A7:3.0% Ce^{3+}, 1.0% Tb^{3+} annealed for 6 hours under a reducing atmosphere is the
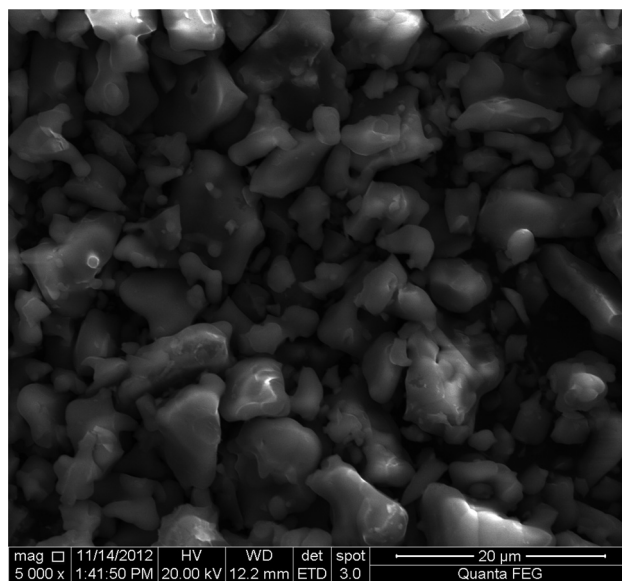

Fig. 9 SEM image of C12A7:3.0% Ce^{3+}, 1.0% Tb^{3+} annealed at 1300 °C for 6 hours under a reducing atmosphere.
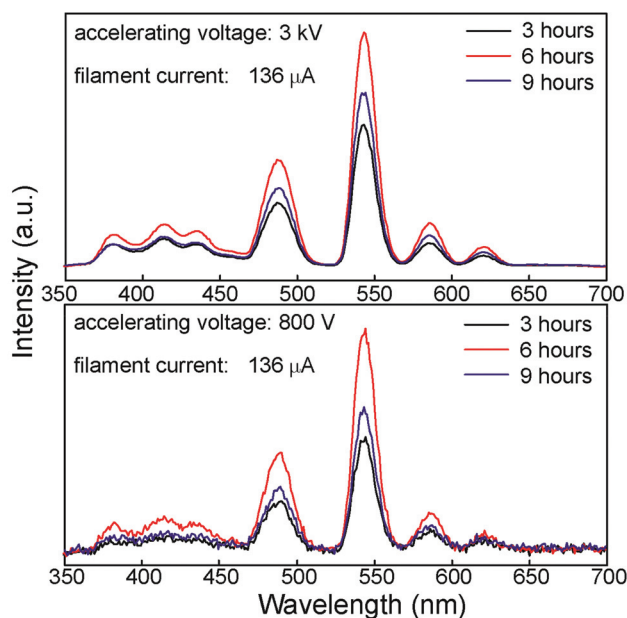
Fig. 10 The CL spectra of C12A7:3.0% Ce^{3+}, 1.0% Tb^{3+} annealed at 1300 °C for different times (3, 6, and 9 hours) under low-voltage (800 V and 3 kV) electron beam excitation.

Fig. 11 CIE chromaticity diagram for C12A7:3.0% Ce^{3+}, 1.0% Tb^{3+} under 5 kV electron beam excitation. The inset shows the CL intensity of C12A7:3.0% Ce^{3+}, 1.0% Tb^{3+} annealed at 1300 °C for 6 hours as a function of accelerating voltage.

strongest one under both 800 V and 3 kV electron beam excitation, which is consistent with its best conductivity according to the optical absorption spectra. It is noteworthy that the CL intensity of the sample increases 60% from 3 to 6 hours reduction treatment under 3 kV excitation, while the improvement is 100% under 800 V electron beam excitation. The results experimentally prove that a better electrical conductivity is more important for the FED phosphor to overcome the charge build-up, especially under low voltage electron beam excitation (<1 kV).

C12A7:3.0% Ce^{3+}, 1.0% Tb^{3+} has the appearance of a spectral green, and the CIE chromaticity coordinates are calculated to be $x = 0.263$ and $y = 0.423$ under 5 kV electron beam excitation, as shown in Fig. 11. The inset shows the CL intensity of the optimal phosphor under electron beam excitation as a function of voltage. The CL intensity increases as the accelerating voltage increases from 1 to 5 kV, which is attributed to the deeper penetration of the electrons into the phosphor. There is no obvious saturation effect observed for the CL at higher accelerating voltages.

A long activator decay time is a factor limiting the attainment of the necessary luminance due to ground state depletion, as found by Stoffers et al.[33] Moreover, a long decay time is thought to be the primary shortcoming of the commercial green phosphor $Zn_2SiO_4:Mn^{2+}$ (11.9 ms) for displaying fast-moving pictures.[34,35] Here, the decay curves of the Tb^{3+} emission monitored at 543 nm for C12A7:0.5% Ce^{3+}, 1.0% Tb^{3+}, C12A7:3.0% Ce^{3+}, 1.0% Tb^{3+}, and $CaCeAl_3O_7$:1% Tb^{3+} were measured as shown in Fig. 12. A single-exponential decay was observed for all the samples, and the values of their lifetimes are fitted to be 2.44, 2.51 and 2.58 ms, indicating that the new
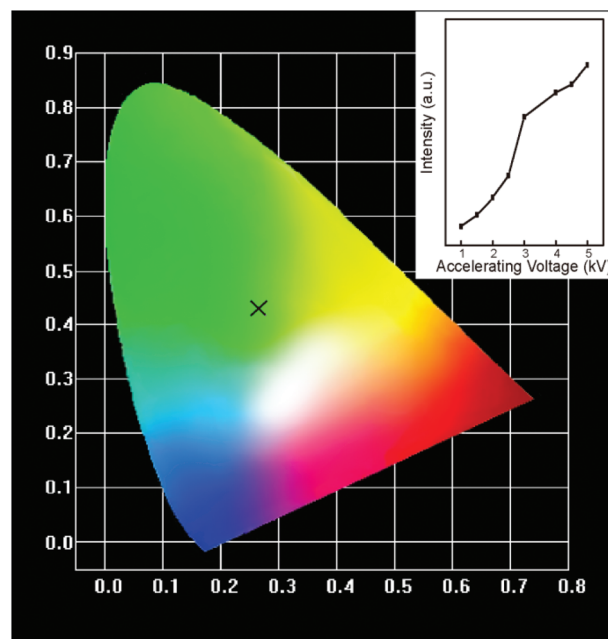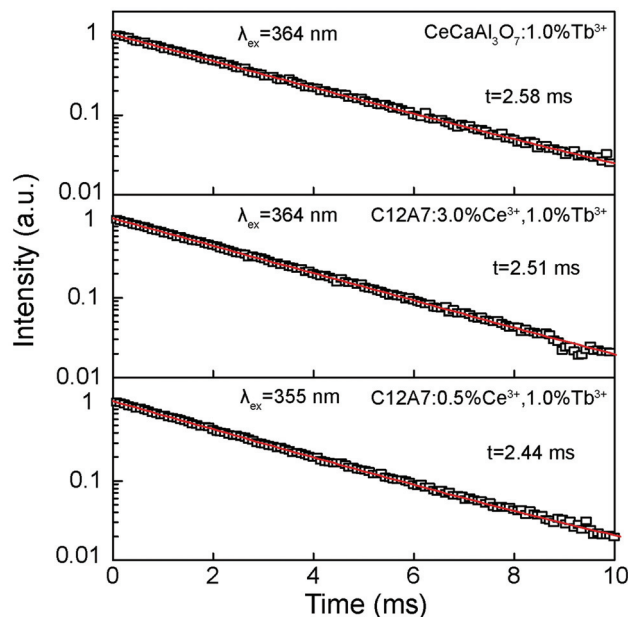

Fig. 12 Decay curves of Tb^{3+} emission monitored at 543 nm for phosphors C12A7:0.5% Ce^{3+}, 1.0% Tb^{3+}, C12A7:3.0% Ce^{3+}, 1.0% Tb^{3+}, and $CaCeAl_3O_7$:1% Tb^{3+}. The red line represents the data best fitted using a single exponential function.

phase $CaCeAl_3O_7$ has no effect on the lifetime of Tb^{3+}. In comparison with $Zn_2SiO_4:Mn^{2+}$, the emission lifetime of our optimized samples, C12A7:3.0% Ce^{3+},1.0% Tb^{3+}, is much shorter, which will improve the display quality for fast-moving pictures.

4. Conclusions

In conclusion, conductive green-light-emitting phosphors $12CaO \cdot 7Al_2O_3$–$CaCeAl_3O_7$:Ce^{3+},Tb^{3+} have been prepared *via* solid-state reactions under a reducing atmosphere. The multiphase strategy broadens the absorption of Ce^{3+}, while efficient energy transfer from Ce^{3+} to Tb^{3+} fully utilizes the absorption of the electronic energy, resulting in the CL enhancement. The CL has been optimized by modifying the electric conductivity and the ratio of C12A7 to $CaCeAl_3O_7$. Our results suggest that the phosphor is a potential green emission candidate for the application of low voltage full-colour FEDs.

Acknowledgements

Notes and references

1 G. Li, X. Zhang, C. Peng, M. Shang, D. Geng, Z. Cheng and J. Lin, *J. Mater. Chem.*, 2011, **21**, 6477.

2 T. Jüstel, H. Nikol and C. Ronda, *Angew. Chem., Int. Ed.*, 1998, **37**(22), 3084.

3 Y. C. Li, Y. H. Chang, Y. F. Lin, Y. J. Lin and Y. S. Chang, *Appl. Phys. Lett.*, 2006, **89**, 081110.

4 F. L. Zhang, S. Yang, C. Stoffers, J. Penczek, P. N. Yocom, D. Zaremba, B. K. Wagner and C. J. Summers, *Appl. Phys. Lett.*, 1998, **72**, 2226.

5 M. Xie, H. Liang, Y. Huang and Y. Tao, *Opt. Express*, 2012, **20**, 15891.

6 D. Geng, G. Li, M. Shang, C. Peng, Y. Zhang, Z. Cheng and J. Lin, *Dalton Trans.*, 2012, **41**, 3078.

7 G. Li, D. Geng, M. Shang, C. Peng, Z. Cheng and J. Lin, *J. Mater. Chem.*, 2011, **21**, 13334.

8 X. Li, J. D. Budai, F. Liu, J. Y. Howe, J. Zhang, X. Wang, Z. Gu, C. Sun, R. S. Meltzer and Z. Pan, *Light: Sci. Appl.*, 2013, e50, DOI: 10.1038/lsa.2013.6.

9 M. Shang, G. Li, D. Yang, X. Kang, C. Zhang and J. Lin, *J. Electrochem. Soc.*, 2011, **158**, J125.

10 M. Shang, G. Li, D. Yang, X. Kang, C. Peng, Z. Cheng and J. Lin, *Dalton Trans.*, 2011, **40**, 9379.

11 M. Zhang, X. Wang, H. Ding, H. Li, L. Pan and Z. Sun, *Int. J. Appl. Ceram. Technol.*, 2011, **8**, 752.

12 S. H. Shin, J. H. kang, D. Y. Jeon and D. S. Zang, *J. Solid State Chem.*, 2005, **178**(7), 2205.

13 C. Y. Shang, H. Kang, H. B. Jiang, S. P. Bu, X. H. Shang and Y. Wu, *J. Lumin.*, 2013, **138**, 182.

14 Y. Toda, Y. Kubota, M. Hirano, H. Hirayama and H. Hosono, *ACS Nano*, 2011, **5**, 1907.

15 K. Hayashi, S. Matsuishi, N. Ueda, M. Hirano and H. Hosono, *Chem. Mater.*, 2003, **15**, 1851.

16 S. W. Kim, T. Shimoyama and H. Hosono, *Science*, 2011, **333**, 71.

17 S. Matsuishi, Y. Toda, M. Miyakawa, K. Hayashi, T. Kamiya, M. Hirano, I. Tanaka and H. Hosono, *Science*, 2003, **301**, 626.

18 S. Matsuishi, T. Nomura, M. Hirano, K. Kodama, S. i. Shamoto and H. Hosono, *Chem. Mater.*, 2009, **21**, 2589.

19 K. Hayashi, Y. Toda, T. Kamiya, M. Hirano, M. Yamanaka, I. Tanaka, T. Yamamoto and H. Hosono, *Appl. Phys. Lett.*, 2005, **86**, 022109.

20 K. Hayashi, S. Matsuishi, T. Kamiya, M. Hirano and H. Hosono, *Nature*, 2002, **419**, 462.

21 X. L. Liu, Y. X. Liu, D. T. Yan, H. C. Zhu, C. G. Liu and C. S. Xu, *J. Nanosci. Nanotechnol.*, 2011, **11**, 9953.

22 *General Structure Analysis System (GSAS)*, ed. A. C. Larson and R. B. Von Dreele, 1994.

23 N. Kodama, T. Takahashi, M. Yamaga, Y. Tanii, J. Qiu and K. Hirao, *Appl. Phys. Lett.*, 1999, **75**, 1715.

24 H. Zhang, H. Yamada, N. Terasaki and C. N. Xu, *J. Electrochem. Soc.*, 2008, **155**, J128.

25 J. Petit, B. Viana, P. Goldner, J. P. Roger and D. Fournier, *J. Appl. Phys.*, 2010, **108**, 123108.

26 L. Zhou, W. C. H. Choy, J. Shi, M. Gong, H. Liang and T. I. Yuk, *J. Solid State Chem.*, 2005, **178**, 3004.

27 S. W. Kim, Y. Toda, K. Hayashi, M. Hirano and H. Hosono, *Chem. Mater.*, 2006, **18**, 1938.

28 D. Jia, R. S. Meltzer, W. M. Yen, W. Jia and X. Wang, *Appl. Phys. Lett.*, 2002, **80**, 1535.

29 W. Chen, Y. Wang, X. Xu, W. Zeng and Y. Gong, *ECS Solid State Letters*, 2012, **1**(4), R17.

30 S. T. Aruna, N. S. Kini, S. Shetty and K. S. Rajam, *Mater. Chem. Phys.*, 2010, **119**, 485.

31 P. V. Sushko, A. L. Shluger, K. Hayashi, M. Hirano and H. Hosono, *Appl. Phys. Lett.*, 2005, **86**, 092101.

32 X. L. Liu, Y. X. Liu, D. T. Yan, H. C. Zhu, C. G. Liu, C. S. Xu, Y. C. Liu and X. J. Wang, *J. Mater. Chem.*, 2012, **22**, 16839.

33 C. Stoffers, S. Yang, F. Zhang, S. M. Jacobsen, B. K. Wagner and C. J. Summers, *Appl. Phys. Lett.*, 1997, **71**, 1759.

34 C. R. Ronda and T. Amrein, *J. Lumin.*, 1996, **69**, 245.

35 M. Xie, H. Liang, B. Han, W. Chen, Q. Su, Y. Huang, Z. Gao and Y. Tao, *Opt. Lett.*, 2009, **34**, 3466.